Structural and magnetic properties of YNi4-xCoxSi alloys

Gai, H.; van Dijk, N.H.; Brück, E.H.

Important note
To cite this publication, please use the final published version (if applicable).
Please check the document version above.

Structural and magnetic properties of YNi$_{4-x}$Co$_x$Si alloys

W. Hanggai [*], N.H. van Dijk, E. Brück

Fundamental Aspects of Materials and Energy (FAME), Faculty of Applied Sciences, Delft University of Technology, Mekelweg 15, Delft 2629JB, the Netherlands

ABSTRACT

The transition-metal based alloy system YNi$_{4-x}$Co$_x$Si shows a second-order ferromagnetic-to-paramagnetic transition near room temperature. Here, the magnetic structure, the magnetocaloric properties and the magnetic anisotropy of YNi$_{4-x}$Co$_x$Si ($x = 0$–4) are investigated. For $x = 3.5$, 3.75 and 4.0 a Curie temperature near room temperature is observed with $T_C = 250$, 283 and 310 K, respectively. In orientated YNi$_{4-x}$Co$_x$Si powder samples the c axis of the hexagonal crystal structure is found to be the easy magnetic axis, with a large dominant K_2 anisotropy constant ($K_2 > K_1 > 0$). The magnetic structure and the preferred atomic position for Ni are demonstrated by neutron diffraction measurements. We have found a dramatic decrease in the magnetic moment at the $3g$ site in the CaCu$_5$-type structure (space group $P6/mmm$), the saturation magnetization and the Curie temperature with increasing Ni concentration.

1. Introduction

Rare-earth alloys can exhibit both a large magnetocaloric effect and hard-magnetic properties [1–5]. The RM_4Si alloys, where R is a rare-earth element (La, Tb, Gd, Y, Tm) and M a 3d transition-metal element (Fe, Co, Ni), form a rich materials family with intriguing physics, including a giant magnetic coercivity, a large magnetocaloric effect and good hydrogen storage properties [6]. The hexagonal CaCu$_5$-type structure (space group $P6/mmm$) shows for some compounds an hexagonal-to-orthorhombic distortion into the orthorhombic YNi$_4$Si-type lattice (space group $Cmmm$), which is a potential route to optimize the magnetocaloric effect [7]. The relation between the lattice parameter in the orthorhombic (O) YNi$_4$Si-type lattice and the hexagonal (H) CaCu$_5$-type lattice is $b_O = (\sqrt{3}\, a_H)$ [8]. In recent years, TbNi$_4$Si ($T_C = 30$ K) and GdNi$_4$Si ($T_C = 25$ K) alloys are reported to show a giant magnetocaloric effect (MCE) at low temperatures [9], but their giant MCE is not optimized to room temperature. In the RNi$_4$Si alloy series a maximum magnetic entropy change was reported to be $|\Delta S_m| = 9.95$ J kg^{-1} K^{-1} for TbNi$_4$Si and $|\Delta S_m| = 12.8$ J kg^{-1} K^{-1} for GdNi$_4$Si in a field change of 5 T [9]. These reports have received much attention for their potential use in green energy-efficient magnetic refrigeration technology and magnetic heat pump applications. In order to make use of this giant MCE in applications, several challenges need to be dealt with: (1) the cost of heavy rare-earth elements brings one of the main challenges for applications, (2) large magnetic field changes are required to achieve the reported MCE effect, (3) the maximum adiabatic

temperature changes at the ferromagnetic transition temperature need to be brought near room temperature. Considering the pronounced sensitivity of the structural and magnetic properties of RM_4Si materials to alloying, it is reasonable to anticipate that these drawbacks can be mitigated through careful adjustment of the chemical composition. First, in the heavy rare-earth ferromagnetic orthorhombic ternary alloys with $M = $ Ni, such as GdNi$_4$Si or DyNi$_4$Si, Gd and Dy occupy the pyramidal sites and carry most of the magnetic moments 7.94 μ_B (Gd) and 10.65 μ_B (Dy), while Ni only carries 0.57 and 0.63 μ_B, respectively [17]. However, in the light rare-earth YNi$_4$Si compound, the theoretical magnetic moment of Y is zero, while the Ni magnetic moment of the above compound is 0.80 μ_B [6]. In order to maximize the magnetic density and the MCE, substitutions with heavy rare-earth elements such as Gd, Dy, Tb should be avoided. Second, in the series of alloys with R fixed to unity, extensive investigations have been carried out on the RNi$_{4-x}$T$_x$Si ($T = $ Co, Fe, Cu, Mn) compounds [9]. The coupling between the 3d transition metals has been identified as a significant factor affecting the magnetic and structural transitions. However, the specific magnetic properties and structural transformations resulting from variations in the ratio of different 3d elements remains unclear. Recent research involving the substitution of heavy rare-earth elements (R) has demonstrated relatively high values for the magnetic saturation polarization ($J_s = \mu_0 M_s$) and the maximum energy product (BH)$_{max}$ at low temperatures [6,9], accompanied by uniaxial magnetic anisotropy [13]. These properties are essential for permanent magnets. Nevertheless, it is important to note that the temperature dependence of magnetization

indicates a complex magnetic transition occurring below the Curie temperature [9].

On the other hand, the effect of substituting Si or Al for one of the Co atoms in YCo$_5$ has been investigated by neutron diffraction and X-ray diffraction, where the Si and Al atoms are found to preferentially occupy the 3g site of the CaCu$_5$-type structure [10–12]. Substitution in YCo$_5$ of Co by Si or Al induces important effects on the magnetic properties: a decrease in the Curie temperature (T_C) and the saturation magnetization (M_S), as well as a change in the magnetic anisotropy. The dilution of the Co sublattice by substitution of the nonmagnetic Al atom for Co decreases the magnetic moment μ_{Co} from 1.6 μ_B to 1.05 μ_B for YCo$_5$ [28] and YCo$_4$Al, respectively. With the substitution of Si for Co, the Co magnetic moment μ_{Co} of the YCo$_4$Si compound dramatically decreases to 0.75 μ_B. Thus, Si and Al substitution have shown a similar trend for their effect on the magnetic properties, although the Co moment μ_{Co} and transition temperature T_C are reduced more strongly by Si substitution compared to Al substitution.

Here, we aim to study a series of Si-based alloys with Y fixed to unity and introduce Co as substitutional element for Ni to explore the magnetic phase transition, in order to understand the evolution of the properties. First Y has no magnetic moment and this can help to better understand specific magnetic properties and structural transformation, resulting from variations in the ratio of different 3d elements. There is also a Si-based compound YCo$_4$Si whose transition temperature is near room temperature. This is one of the key conditions for magnetic heat pump applications. Therefore, the main focus of this study is on the quantitative evaluation of magnetic anisotropy parameters and magnetic phase transitions in YNi$_{4-x}$Co$_x$Si compounds.

2. Experimental details

The YNi$_{4-x}$Co$_x$Si compounds have been prepared by melting high-purity starting elements Y (99.9%), Ni (99.98%), Co (99.8%) and Si (99.9%) in an arc melting furnace under a purified argon atmosphere. The molten ingots were turned and remelted five times to ensure homogeneity. Then the as-cast ingots were put into a quartz tube with a nozzle at the bottom, melted and ejected through the nozzle onto a cold Cu wheel rotating at a surface speed of 36 m/s. The thickness of the melt spun ribbons was 20–40 µm. To ensure the samples are single-phase, we added 3% of yttrium to compensate for oxides in the starting material. To explore the impact of the heat treatment on the crystal structure, we subjected the YNi$_{4-x}$Co$_x$Si compounds that were sealed in quartz ampoules filled with Ar, to an annealing at 873 K for 24 h, followed by rapid quenching in ice-cold water. The structure, purity and composition of the polycrystalline samples were evaluated using powder X-ray diffraction (XRD), electron microscopy and energy dispersive spectroscopy (EDS). The X-ray data are obtained on a PANalytical X-Pert PRO diffractometer (Cu-K_α radiation, angular range 10°- 90°, angular step 0.02°, 1 s per step). The temperature- and field-dependent magnetization was measured with a superconducting quantum interference device (Quantum Design MPMS-XL) at a ramp rate of 2 K/min using the reciprocating sample option (RSO). The sample mass for the SQUID magnetisation experiments was approximately 1–2 mg. Neutron diffraction (ND) experiments were carried out at the research reactor of the TU Delft [14]. A neutron wavelength of 1.67 Å was selected by the (5 3 3) reflection of a germanium single crystal monochromator. The powder samples with a mass of 5 g were loaded under argon in a 6 mm diameter air-tight vanadium sample can (wall thickness of 100 µm). The data were collected at temperatures of 5, 298 and 350 K. Refinements of the diffraction data were performed using the Rietveld method [15] as implemented in the Fullprof software [16]. Field-oriented samples were prepared by solidifying a mixture of glue and powdered specimen in a magnetic field of 1 T in the ferromagnetic state. Prior to orienting in field, the samples were powdered and then sieved down to a particle size smaller than 30 µm.

3. Results and discussion

3.1. Crystalline structure

X-ray diffraction analysis confirms that the as-cast YNi$_{4-x}$Co$_x$Si compounds crystallize in the hexagonal CaCu$_5$-type structure (space group *P6/mmm*). Both X-ray diffraction and EDS shows that the YNi$_{4-x}$Co$_x$Si compounds are single phase, as shown in Fig. 1a. The unit cell includes the 1a site (0,0,0) for Y and the two different crystallographic positions 2c (1/3,2/3,0) and 3g (1/2,0,1/2) for Co, Ni and Si, where the Ni and Si atoms predominantly occupy the 3g site [10,12]. The 2c site lies within the same plane as the 1a site, while the 3g position is positioned halfway in between the layers containing the 2c and 1a sites. In YNi$_{4-x}$Co$_x$Si compounds the lattice parameters a and c show an opposite trend when Co substitutes Ni, with an increase in unit-cell volume for an increasing Co content x. The c/a ratio decreases for an increasing Co content, as shown in Fig. 1c and Table 1.

The CaCu$_5$-type hexagonal phase was not detected in the annealed YNi$_4$Si compound, which crystallizes in YNi$_4$Si-type orthorhombic phase (space group *Cmmm*). The unit cell includes the 2c site (1/2,0,1/2) for Y, the 2a site (0,0,0) for Si and the two different crystallographic positions 4j (0,0.15,1/2) and 4e (1/4,1/4,0) for Ni. Fig. 1d, reveals the orthorhombic distortion of the CaCu$_5$ structure (as-cast sample), in line with the report by Morozkin and coworkers [6]. The $b_O/\sqrt{3}a_H$ ratio can be used to estimate the degree of distortion. The obtained value of $b_O/\sqrt{3}a_H$ = 1 corresponds to the transformation of the hexagonal CaCu$_5$-type lattice into the orthorhombic YNi$_4$Si-type lattice [8]. In the present results, only the YNi$_4$Si compound shows a clearly different structure between the as-cast and annealed samples with $b_O/\sqrt{3}a_H$= 0.97016(8) at room temperature (298 K). After Co substitution for Ni, the studied YNi$_{4-x}$Co$_x$Si (x =1–2) compounds show a disordered orthorhombic phase, which may be viewed as the disordered variant of the YNi$_4$Si-type structure (mixed occupancy of the 2c, 4f and 4i sites in the orthorhombic lattice) [9]. The YNiCo$_3$Si and YCo$_4$Si compounds do not show a disordered phase after annealing. In our results the disordered structure exists until 50% Co substitution (x = 2). The temperature for the appearance of the distorted phase strongly depends on the Co concentration. Therefore, in this study we mainly focused on intrinsic physical properties of the as-cast YNi$_{4-x}$Co$_x$Si (x = 0-4) compounds with the hexagonal structure.

3.2. Magnetic phase transition

From the temperature- and field-dependent magnetization in Fig. 2a, b we note that a substantial increase in the ferromagnetic transition temperature (T_C) and the saturation magnetization (M_S) is evident upon substituting Co for Ni. For YNi$_{4-x}$Co$_x$Si (x = 2–4), a ferromagnetic-to-paramagnetic transition without thermal hysteresis is observed. In the insert of Fig. 2a, it can be seen that for the parent YNi$_4$Si compound a paramagnetic behaviour is found in the complete temperature range from 5 to 370 K. For YNi$_4$Si the effective magnetic moment μ_{eff} obtained from the Curie-Weiss law is 0.3 μ_B/f.u. [8,9]. As shown in the insert of Fig. 2b the field-dependent magnetization of YNi$_4$Si shows a magnetization per formula unit ($M_{5\,T}$) of 0.01 μ_B/f.u. in a field of 5 T ($1/H \rightarrow$ 0 gives $M_\infty \rightarrow$ 0.02 μ_B/f.u.). These observations suggest a negligible Ni magnetic moment in YNi$_4$Si compounds. The nearly filled Ni (3d) band implies that the Ni magnetic moment is negligible [17,18]. For the YNi$_3$CoSi compound the field-dependent magnetization measurements at 5 K show an unusual ferrimagnetic behaviour without a saturation in fields up to 5 T with $M_{5\,T}$ = 0.03 μ_B/f.u. ($1/H \rightarrow$ 0 gives $M_\infty \rightarrow$ 0.04 μ_B/f. u.). This indicates that the magnetic moments are enhanced with partly antiferromagnetic (or more complex) spin orientations. A enlargement of the weak magnetization curve for YNi$_3$CoSi is shown in the inset of Fig. 2b.

Fig. 2c shows T_C and M_S as a function of the Co content, indicating
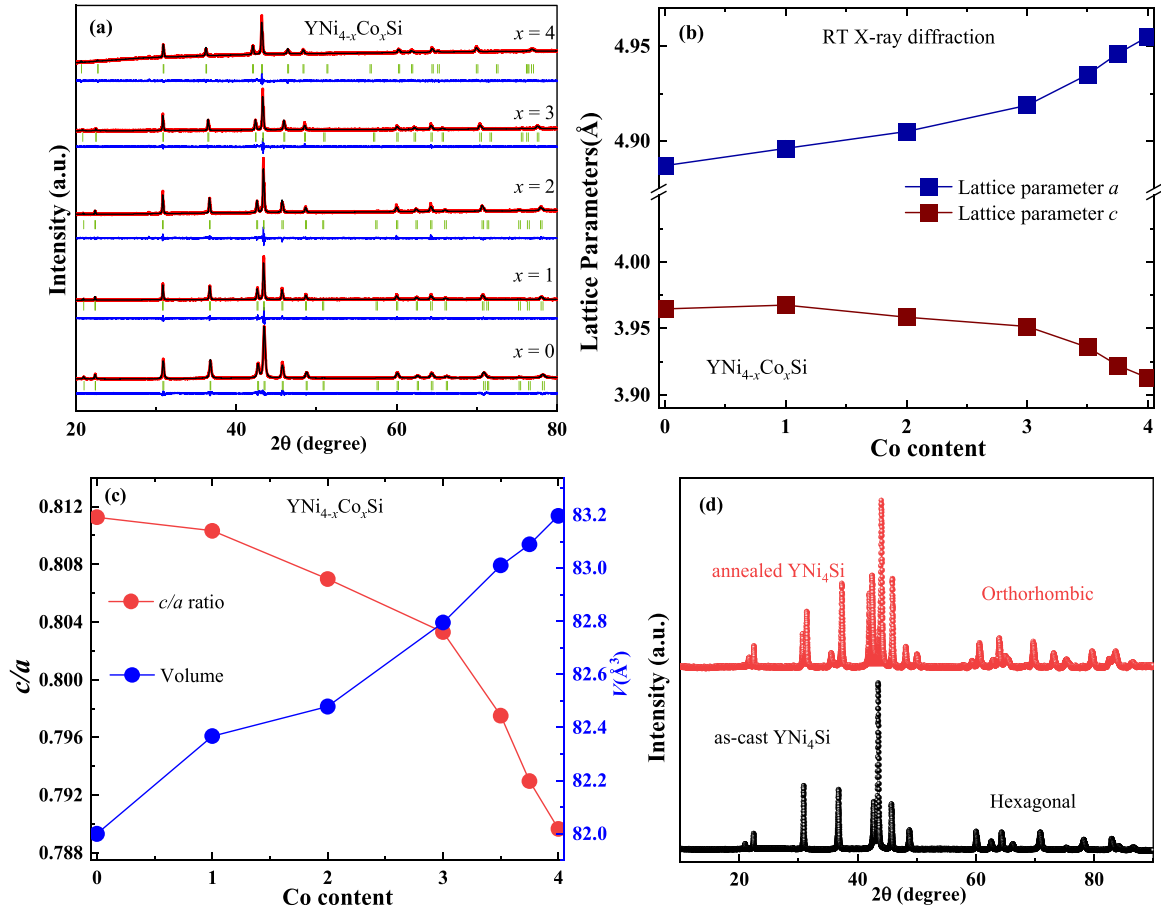
Fig. 1. (a) X-ray powder diffraction patterns of the YNi$_{4-x}$Co$_x$Si alloys at room temperature. (b) Lattice parameters of the hexagonal phase in the YNi$_{4-x}$Co$_x$Si compounds as a function of the Co content x. (c) Unit-cell volume and c/a ratio of the YNi$_{4-x}$Co$_x$Si compounds as a function of the Co content x. (d) CaCu$_5$-type hexagonal phase of the as-cast YNi$_4$Si compound and the YNi$_4$Si-type orthorhombic phase of the YNi$_4$Si compound after annealing at 873 K.

Table 1
Lattice parameters a and c, c/a ratio and unit-cell volume V obtained by room-temperature XRD, saturation magnetization M_s and Curie temperature T_C for the YNi$_{4-x}$Co$_x$Si ($2 \leq x \leq 4$) compounds. M_s is obtained from magnetisation measurements at 5 K and T_C from magnetisation measurements in an applied field of 0.01 T.

x	a (Å)	c (Å)	c/a	V (Å^3)	M_s (Am^2 kg^{-1})	T_C (K)	$\Delta S_{M,max}$ (Jkg^{-1}K^{-1})
0.0	4.88695 (6)	3.96460 (6)	0.81126 (1)	81.998 (2)	-	-	-
1.0	4.89615 (7)	3.96746 (7)	0.81032 (2)	82.367 (2)	-	-	-
2.0	4.90510 (8)	3.95833 (7)	0.80698 (2)	82.478 (3)	4.61	32	0.18
3.0	4.91887 (9)	3.95132 (8)	0.80330 (2)	82.795 (3)	21.51	150	0.29
3.5	4.9350 (13)	3.93569 (11)	0.79750 (3)	83.010 (4)	31.54	250	0.60
3.75	4.9459 (14)	3.92199 (12)	0.79296 (3)	83.089 (4)	36.83	283	0.66
4.0	4.9550 (13)	3.91280 (13)	0.78967 (3)	83.196 (4)	42.67	310	0.75

that the transition temperature T_C increases from 32 to 310 K in the YNi$_{4-x}$Co$_x$Si (x = 2–4) compounds and can continuously be varied near room temperature by adjusting the Ni/Co ratio. Since the temperature dependence of the magnetization exhibits a relatively broad transition, the transition temperature defined as the maximum in the first derivative $|dM/dT|$ is not necessarily accurate. However, the mean field models are an alternative option for predicting transition temperature. Therefore, we used the equation $M(T)^2 = A^2(T_C - T)$ to estimate T_C (Table 1). For a Co concentration above 50% ($x > 2$), a strong increase in saturation magnetization is observed from 5 (x = 2) to 43 (x = 4) Am^2/kg. The isothermal magnetic entropy change is calculated by applying the Maxwell relation $\Delta S_M(T)_{\Delta H} = \int_{Hi}^{Hf} \mu_0 \left(\frac{\partial M(T,H)}{\partial T}\right)_H dH$ [20,21] to the M(T) data at different fields. The magnetic or indirect calorimetric determinations of the entropy change suffer from uncertainties, typically of the order of 10% [22]. As indicated in Fig. 2d, the YNi$_{0.5}$Co$_{3.5}$Si,

YNi$_{0.25}$Co$_{3.75}$Si and YCo$_4$Si compounds (x = 3.5, 3.75, 4.0) show a maximum $|\Delta S_m|$ of 0.60, 0.66 and 0.75 J kg/K for a field change of 3 T, respectively. While the values for the magnetic entropy change are limited, the magnetocaloric effect is spread out over a wide temperature range due to the broadening of the $M(T)$ curve in higher magnetic fields. Typically, this behaviour is observed in magnetocaloric materials with a second-order magnetic phase transition as a result of the temperature- and field-dependence of the magnetocaloric effect. To get further insight into the order of the ferromagnetic transition in YCo$_4$Si, we used a method recently proposed by Franco and coworkers [23,24]. Assuming that the field-dependence of the isothermal magnetic entropy change follows a power law of the type $|\Delta S_m| \propto H^n$. The field exponent $n = \frac{d\ln(|\Delta S_m|)}{d\ln(H)}$ generally shows a significant variation near the transition temperature [24,25]. In particular, $n > 2$ was proposed for materials characterized by a first-order magnetic phase transitions (FOPT). Fig. 3
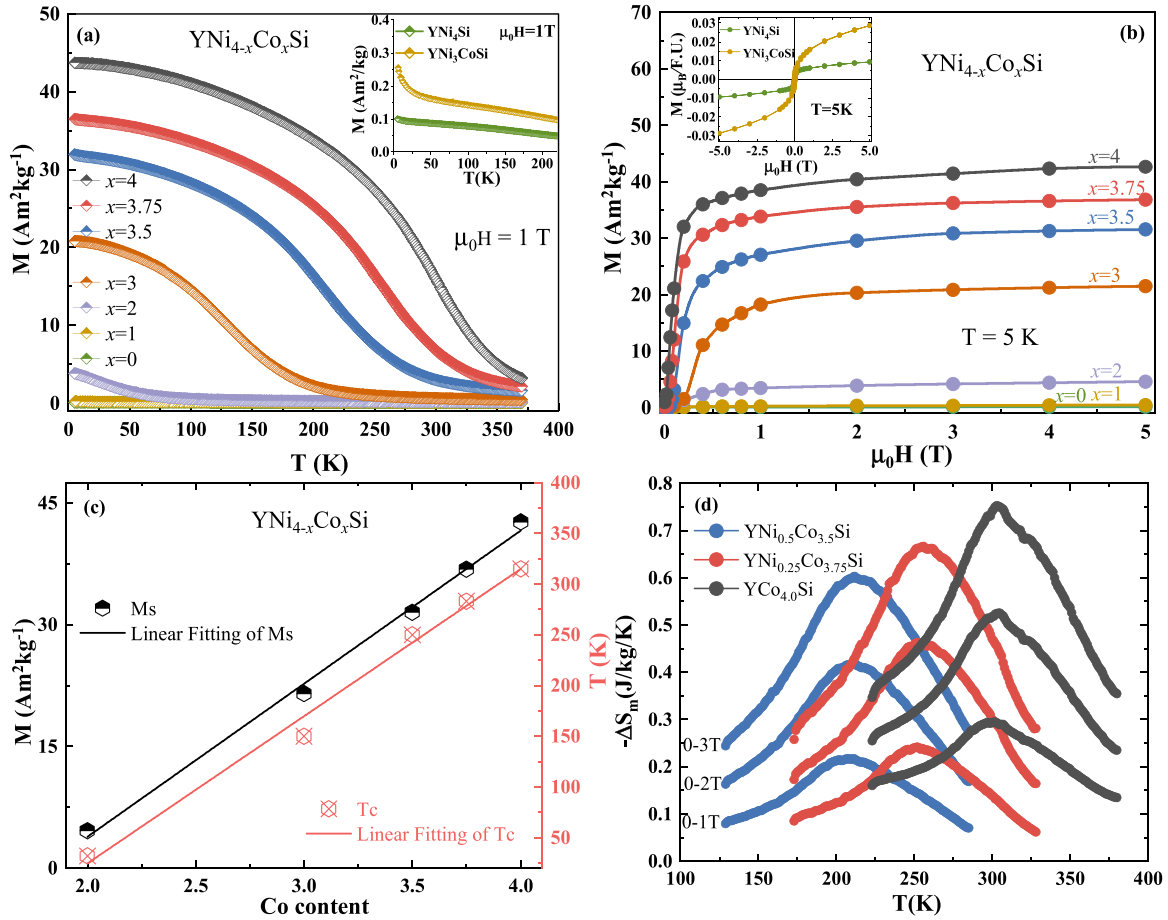
Fig. 2. (a) Magnetization as a function of temperature in an applied field of 1 T and (b) magnetization as a function of magnetic field at 5 K of $YNi_{4-x}Co_xSi$ ($x = 0–4$) (inset shows an enlargement of the weak magnetisation curves for $x = 0–1$). (c) Values of T_C and M_s for $YNi_{4-x}Co_xSi$ ($x = 0–4$) as a function of the Co content. (d) Isothermal entropy change $-\Delta S_m$ obtained from the magnetisation $M(T)$ upon heating in a field change of 1, 2 and 3 T.
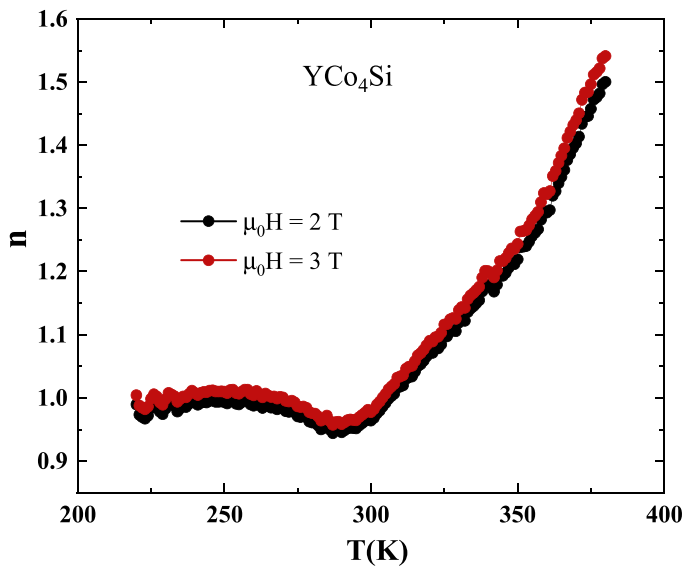
Fig. 3. Field exponent n of the magnetic entropy change in a field change of 2 and 3 T.

shows the local field dependence of the isothermal magnetic entropy change (ΔS_m) for the YCo_4Si compound. It is clearly seen that $n < 2$ near T_C for $\Delta\mu_0 H = 2$ and 3 T, reflecting a second-order magnetic phase transition (SOPT) [24]. Similar results were obtained for the other Ni/Co

compounds ($x = 3.5, 3.75, 4$). In a conventional paramagnet ($T > T_C$) the value of n tends to 2. The analysis of the field dependence of ΔS_m thus demonstrates the SOPT character of the ferromagnetic transition. This is consistent with the absence of thermal hysteresis in the $M(T)$ curves for these materials.

To study the characteristics of the magneto-elastic coupling, high-resolution XRD measurements are performed as function of temperature. Fig. 4a shows that the (111) reflection for the YCo_4Si compound shifts to a smaller angle at higher temperature as a result of the magnetic transition. This behaviour is linked to the magneto-elastic coupling of the magnetic order with the thermal expansion of the lattice. Fig. 4b shows the unit-cell volume as a function of temperature in the temperature range from 150 to 400 K. Due to the magnetic phase transition the linear continuous change in volume shows a kink at the ferromagnetic transition temperature (310 K). The volume difference ΔV between the ferromagnetic state and the linear extrapolation of the paramagnetic state can be regarded as the contribution from the magneto-elastic coupling. The transition temperature determined from the temperature-dependent XRD is in agreement with the transition found in the magnetization. The value is in agreement with the transition temperature of 320(5) K reported by Isard and coworkers for the YCo_4Si compound [10] and is lower than the value of $T_C = 350$ K reported by Thang and coworkers [26].

3.3. Magneto-crystalline anisotropy

To highlight the significant magneto-crystalline anisotropy in the quaternary $YNi_{4-x}Co_xSi$ compounds, we selected three representative
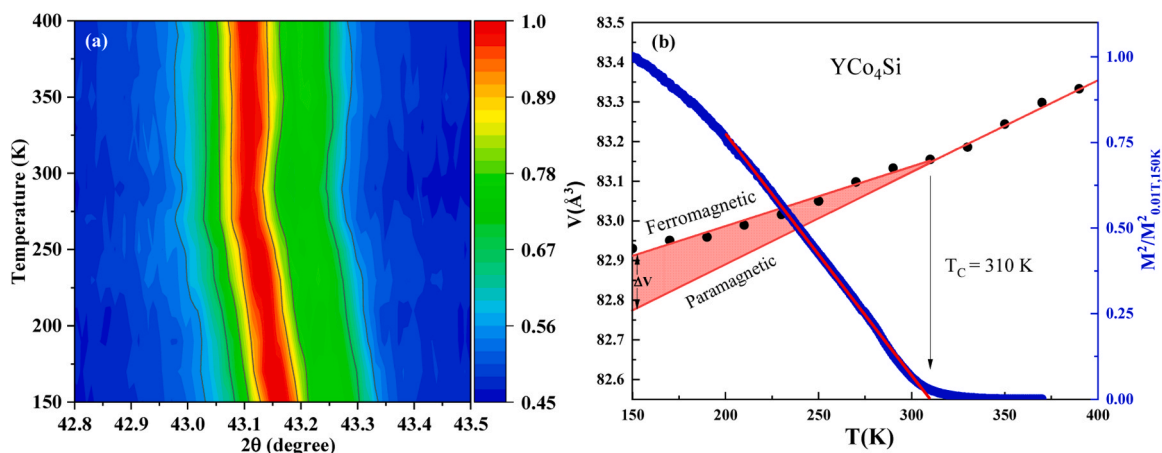
Fig. 4. (a) (111) reflection of YCo$_4$Si as a function of temperature. (b) Temperature dependence of the unit-cell volume V and the normalized M^2-T curve in a magnetic field of 0.01 T for the YCo$_4$Si compound.

polycrystal samples ($x = 3.5$, 3.75 and 4.0) with a T_C near room temperature and hand crushed them into particles with a size smaller than 30 μm. During the field orientation process the powder was mixed with glue and placed on a plate in a magnetic field of 1 T orientated perpendicular to the plate.

XRD measurements were performed on the surface of the plate. The XRD measurements show a large difference between the results for field-oriented powders and free powders. Due to the magnetic orientation,

one observes in Fig. 5a that reflections with a or b axis components, like (1 1 0) and (2 0 0), disappear almost completely. Simultaneously, reflections with a pure c axis component, like (0 0 1) and (0 0 2), are strongly enhanced. This indicates that in polycrystalline YNi$_{4-x}$Co$_x$Si (x = 3.5–4) compounds the c-axis is the easy magnetization direction (EMD), and the a-b plane is a hard magnetization direction (HMD). This result is in agreement with previous studies on YCo$_5$, YCo$_4$Al, YCo$_{4.5}$Ge$_{0.5}$ and YCo$_4$B [11,27–29]. The YCo$_4$B compound however
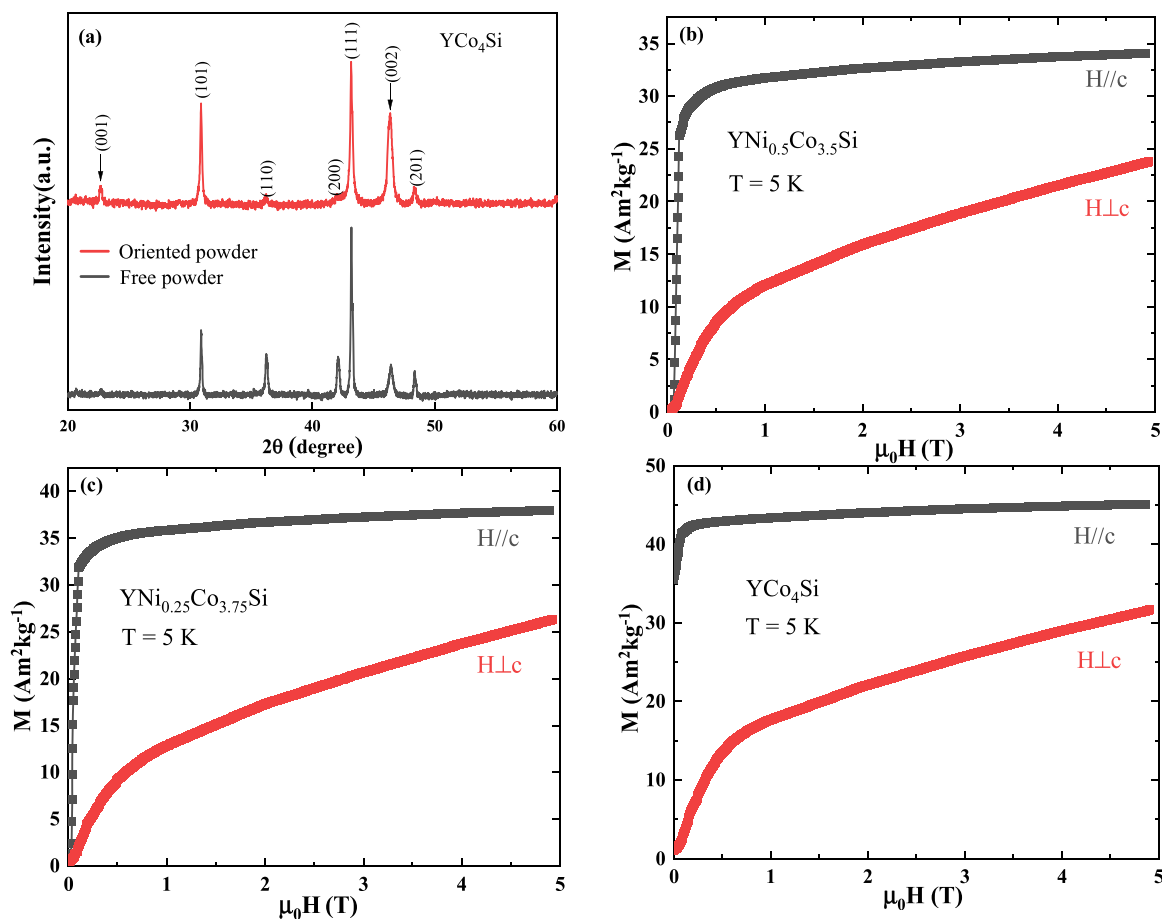
Fig. 5. (a) comparison between field-oriented and free powder XRD indicating large changes in the peak intensities by the alignment of the easy axis along the applied field. (b - d) Magnetization as a function of field for the YNi$_{4-x}$Co$_x$Si (x = 3.5, 3.75 and 4.0) compounds measured parallel and perpendicular to the c axis of the hexagonal lattice at 5 K.

shows a spin reorientation at low temperature (150 K) with the EMD in the *a-b* plane below the spin reorientation temperature [19,27].

Isothermal magnetization curves were systematically recorded in all quadrants and reveal magnetic hysteresis loops with a significant coercive field at low temperature. In Fig. 5(b-d) only the first quadrant measurements were performed at 5 K along the *c* axis and in the *a-b* plane for each compound. The $M(H)$ curves measured at low temperature (5 K) clearly indicate a particularly large magnetic anisotropy, as the anisotropy field ($\mu_0 H_{an}$) is significantly higher than our applied field of 5 T. A linear extrapolation suggests that $\mu_0 H_{an}$ is of the order of 10 T, which is half of the value $\mu_0 H_{an} = 20$ T obtained for YCo$_{4.5}$Ge$_{0.5}$ [29]. This anisotropy slowly decreases with increasing temperature until it approaches the Curie temperature where it decreases more rapidly and finally vanishes. As shown in Fig. 6 the coercive field of YCo$_4$Si significantly reduces from 160 kA/m at 5 K to 0.55 kA/m at 300 K. The RM_5-type materials exhibit relatively large values for the saturation magnetic polarization $J_s = \mu_0 M_s$, the maximum energy product $(BH)_{max}$, and the uniaxial magnetic anisotropy, with the hexagonal *c* axis serving as the easy magnetic direction [6,9]. These properties are of utmost importance for the development of permanent magnets. The insert in Fig. 6 shows the $B(H)$ hysteresis measurements at 5 K (including the virgin magnetization curve). It can be seen $(BH)_{max}$ of the present YCo$_4$Si compound is 19 kJ m^{-3} at 5 K (it is 1.0 kJ m^{-3} at 200 K). The saturation magnetic polarization J_s is listed in Table 2. Polarized neutron diffraction experiments [28] have demonstrated that the high anisotropy in YCo$_5$ is associated with an important orbital contribution on the Co 2*c* site. As reported by Pareti and coworkers [30] the CaCu$_5$ -type structure contains two different Co sites: 2*c* and 3*g*. These two Co sites give opposite contributions to the magneto-crystalline anisotropy: axial for 2*c* and planar for 3*g* [11,28,30,33]. The overall axial anisotropy of YCo$_5$ is the sum of the two contributions. Therefore, it deserves a study dedicated to other 3*d* metals substitutions (often considered are Cu, Ni and Fe).

In order to calculate the anisotropy constant, first the effect of the demagnetizing field was included assuming an internal field $H_{in} = H_{ap} - NM$, where H_{ap} is the applied magnetic field, M the magnetization and N the sample-shape dependent demagnetizing factor. For an uniaxial

Table 2

Comparison of the magnetocrystalline anisotropy constants K_1 and K_2, saturation specific magnetization (M_s), saturation magnetic polarization ($J_s = \mu_0 M_s$) and coercive field H_C for the YNi$_{4-x}$Co$_x$Si ($x = 3.5$, 3.75 and 4.0) compounds.

Material	K_1 (5 K) (MJ m^{-3})	K_2 (5 K) (MJ m^{-3})	M_s (5 K) (μ_B/f.u.)	J_s (5 K) (T)	H_C (5 K) (kA m^{-1})
YCo$_4$Si	0.18(1)	1.05(2)	2.69(1)	0.41(2)	160(1)
YCo$_{3.75}$Ni$_{0.25}$Si	0.34(2)	0.98(3)	2.32(2)	0.37(2)	143(3)
YCo$_{3.5}$Ni$_{0.5}$Si	0.38(1)	0.89(3)	1.99(2)	0.36(1)	135(1)

system the magnetic anisotropy constants are K_1 and K_2. The magnetocrystalline anisotropy energy E_A in a crystal can be expressed as $E_A \approx K_1 \sin^2\theta + K_2 \sin^4\theta$, where θ is the angle between the magnetization vector and the axial symmetry direction of the crystal (in this case *c* axis for the hexagonal lattice). The K_1 and K_2 magnetocrystalline anisotropy constants can be estimated from the magnetization curves recorded parallel and perpendicular to the *c* axis in the temperature range from 5 to 350 K, using the Sucksmith and Thompson method [31]. In this method the following relation is considered: $\frac{2K_1}{J_s^2} + \frac{4K_2}{J_s^4}J^2 = \frac{H}{J}$, where $J = \mu_0 M$ is the magnetic polarization and H the internal magnetic field. Fig. 7 presents the obtained temperature evolution of K_1 and K_2 for each compound. The values at low temperature (5 K) are listed in Table 2. The K_1 and K_2 magnetic anisotropy values are both positive, as is expected for materials with a *c* easy magnetization axis (an easy axis is predicted under the condition that $K_1 > 0$ and $K_2 > -K_1$). For all three alloys we find $K_2 > K_1 > 0$. For YCo$_4$Si we find $K_1 \approx 0.18$ MJ m^{-3} and $K_2 \approx 1.05$ MJ m^{-3} at 5 K. The K_2/K_1 ratio decreases for increasing Ni substitutions. As expected, the magneto-crystalline anisotropy constants K_1 and K_2 decrease for increasing temperature and vanish at T_C.

3.4. Magnetic structure

Powder neutron diffraction (ND) is a powerful method to determine the magnitude and direction of magnetic moments. A precise structure determination of the Ni location in the CaCu$_5$-type structure was completed by powder ND investigations. For YCo$_4$Si the 1*a* site is
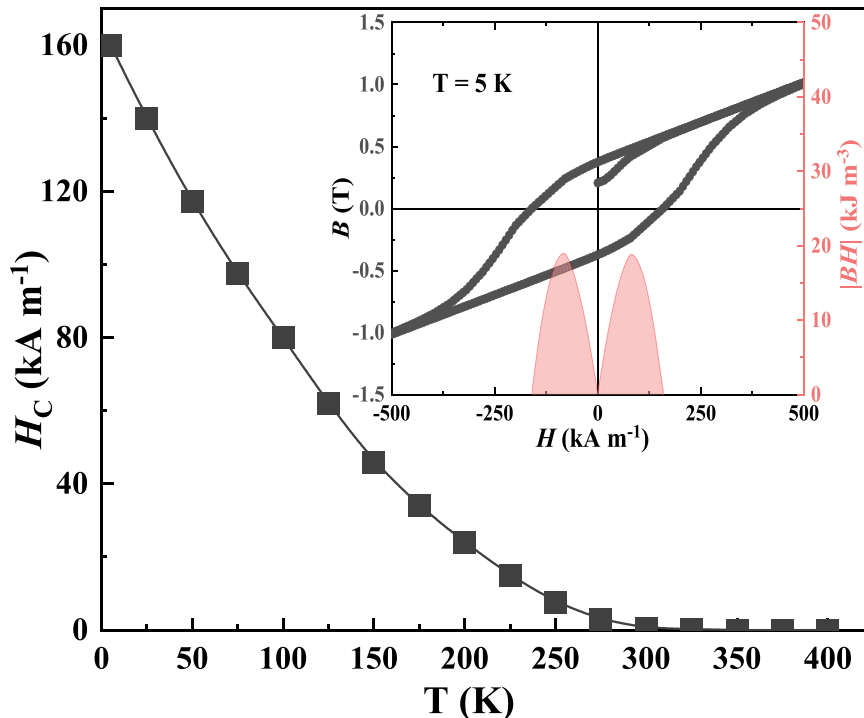
Fig. 6. Coercive field H_C versus temperature for field-oriented YCo$_4$Si powder. The insets shows the $B(H)$ hysteresis measurements at 5 K.
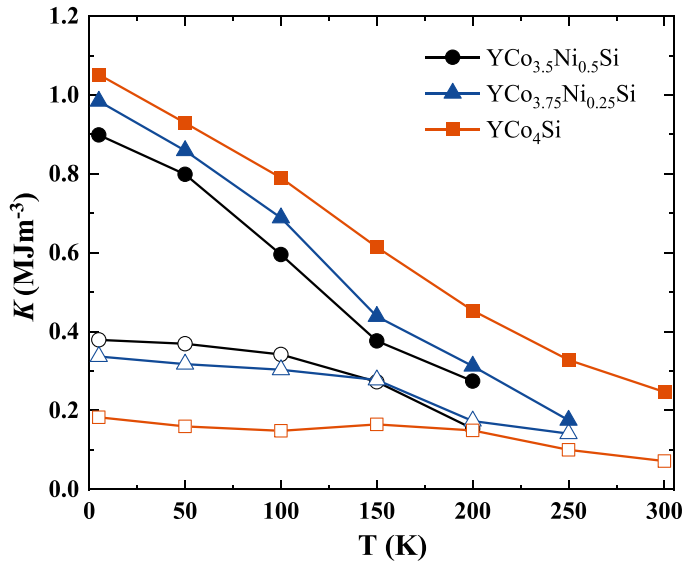
Fig. 7. Magneto-crystalline anisotropy constants K_1 (open symbols) and K_2 (full symbols) determined as a function of the temperature by the Sucksmith and Thompson method for $YNi_{4-x}Co_xSi$ (x = 3.5, 3.75 and 4.0).

occupied by Y and the 2c and 3g sites are occupied by Co and Si. It is well known that in the RCo_5 structure the Si atoms preferentially occupy the 3g site [10,32,33]. Fig. 8a shows a comparison of the neutron diffraction pattern of YCo_4Si at 5 and 350 K. No new peaks appear in the ferromagnetic (FM) state in comparison with the paramagnetic (PM) state of YCo_4Si. Therefore, the propagation vector of the magnetic structure corresponds to $\mathbf{k} = (0,0,0)$. From the enhancement of the peak intensity of the (100) and (201) reflections and the absence of an enhancement for the (002) reflection it can be deduced that the spins in the FM state are aligned along the c-axis. Thus, the irreducible representation used for the magnetic basic vector is $\Phi = (0\ 0\ 1)$. The refinement of the neutron patterns shown in Fig. 8b confirm the hexagonal $CaCu_5$-type structure (space group $P6/mmm$) for all compounds. This is in line with the XRD results. For the YCo_4Si compound magnetic moments of $0.56\mu_B$ on the 2c site and $0.58\mu_B$ on the 3g site have been found. These values are almost equal, as was found for the YCo_4Ga compound by Thang and coworkers [11]. The sum of the Co magnetic moments (2.86(7) μ_B/f.u.) is slightly larger than the value obtained by bulk magnetization (2.69 μ_B/f.u.) in the present results. The total magnetic moment obtained from neutron diffraction 2.86(7) μ_B/f.u. is comparable with the value of 3.0 μ_B/f.u. reported by Isnard and coworkers [10] and obtained by SPR-KKR calculations reported by Benea and coworkers [34].

After a partial Ni substitution for Co, the Ni atoms preferentially occupy the 3g site. As a result, the magnitude of the magnetic moments on the 3g site decreases more rapidly compared to the 2c site. For instance, as shown in Fig. 8c and Table 3 the magnitude of the Co-3g magnetic moment ($0.27\mu_B$) is only about half of that obtained on the Co-
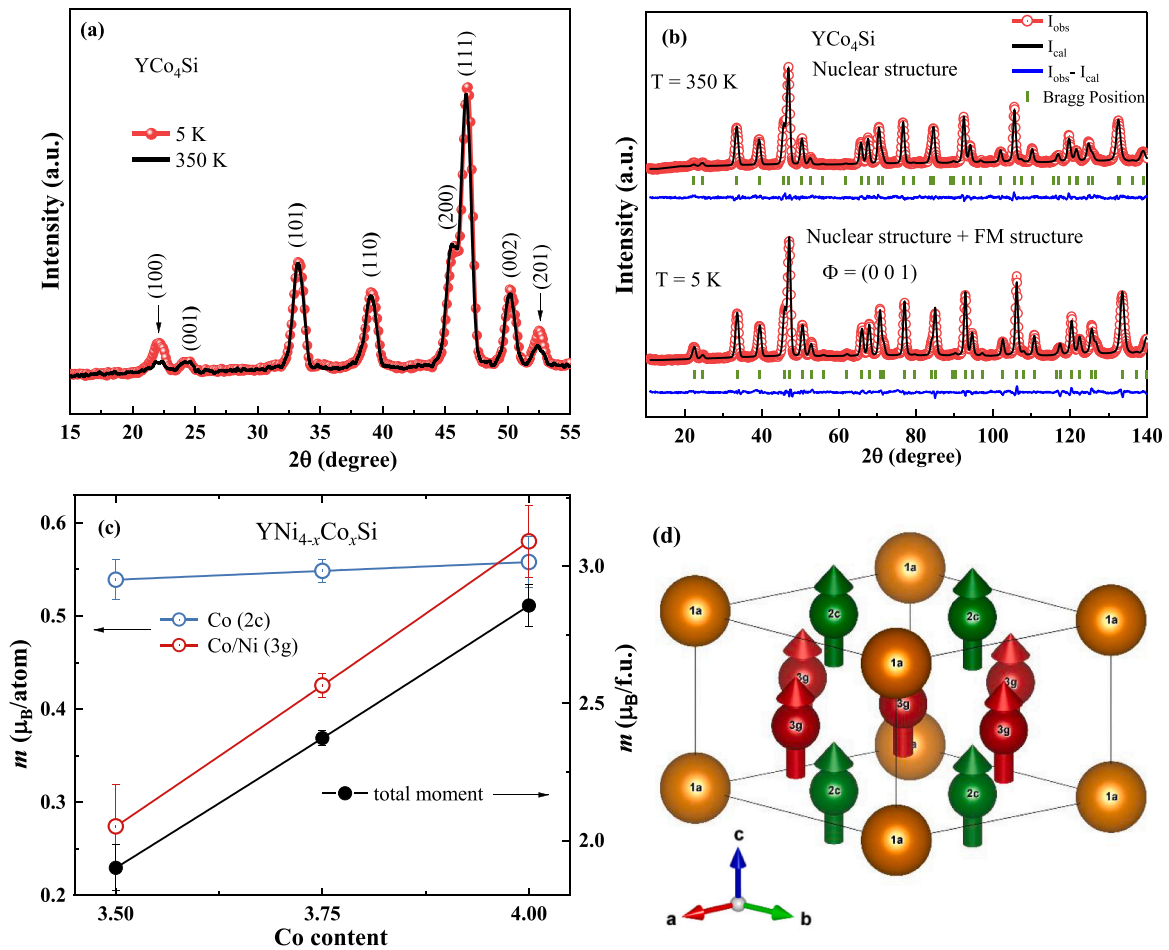
Fig. 8. Powder neutron diffraction pattern of $YNi_{4-x}Co_xSi$ obtained at 5 and 350 K. (a) Comparison of the YCo_4Si compound in the ferromagnetic state (5 K) and in the paramagnetic state (350 K). (b) Refinements of the nuclear and magnetic structure. (c) Magnetic moment of the $YNi_{4-x}Co_xSi$ (x = 3.5, 3.75 and 4) compounds obtained by neutron diffraction at 5 K. (d) Magnetic structure of the YCo_4Si compound in the ferromagnetic state, the moments are aligned along the c axis.

Table 3

Results of the neutron diffraction data analysis for $YNi_{4-x}Co_xSi$ ($x = 3.5$, 3.75 and 4.0) at 5 K.

Parameters	YCo$_4$Si (5 K)	YCo$_{3.75}$Ni$_{0.25}$Si (5 K)	YCo$_{3.5}$Ni$_{0.5}$Si (5 K)
a (Å)	4.93395 (5)	4.92382 (4)	4.91219 (3)
c (Å)	3.90145 (7)	3.91145 (6)	3.92268 (5)
V (Å^3)	82.252 (2)	82.125 (2)	81.972 (1)
easy magnetization axis	c axis	c axis	c axis
μ_{Co-2c} (μ_B)	0.5580 (272)	0.54849 (127)	0.539 (216)
μ_{Co-3g} (μ_B)	0.58028 (384)	0.42549 (127)	0.27411 (451)
M (μ_B/f.u.)	2.85684 (768)	2.37345 (284)	1.90033 (838)
2c site (%Co)	100 (2)	100 (2)	100 (2)
3g site (%Co)	63 (3)	56 (3)	50 (3)
d_{2-2c} (Å)	2.84863(3)	2.84278(2)	2.83607(2)
d_{3-3g} (Å)	2.46697(3)	2.46191(2)	2.45610(2)
d_{1a-1a} (Å)	3.90145(7)	3.91145(6)	3.92268(5)
d_{2c-3g} (Å)	2.41536(3)	2.41768(3)	2.42025(2)
d_{1a-2c} (Å)	2.84863(3)	2.84278(2)	2.83607(2)
d_{1a-3g} (Å)	3.14504(2)	3.14418(2)	3.14313(2)
R_{exp}, R_{wp}, R_p (%)	3.14, 8.80, 10.7	4.06, 9.27, 10.7	4.03, 8.33, 9.36

2c site (0.54μ_B) in the YNi$_{0.5}$Co$_{3.5}$Si compound. However, we observe a rather constant (within 0.01μ_B) contribution of the Co-2c magnetic moments at low temperature (5 K) for the three different compounds. Fig. 8d shows a representative magnetic unit cell for YNi$_{4-x}$Co$_x$Si compounds. The number of formula units $Z = 1$, indicates the presence of 1 formula unit contained within the unit cell. In YNi$_{4-x}$Co$_x$Si compounds the nuclear unit cell has the same size as the magnetic unit cell and the magnetic moments are aligned with the c axis. This alignment serves as a dual confirmation that the YNi$_{4-x}$Co$_x$Si compounds are uniaxial systems with the c axis as easy magnetization axis. Furthermore, the replacement of Ni leads to a marginally reduced atomic separation between the Co atoms at the d_{2c-2c} and d_{3g-3g} spacings. The specific atomic distances between various atomic positions can be found in Table 3.

4. Conclusions

YNi$_{4-x}$Co$_x$Si ($x = 0$–4) compounds were synthesised and characterized to investigate their magnetic properties. By analysing the field dependence of the magnetocaloric effect, it was found that the ferromagnetic-to-paramagnetic transition is a second-order magnetic phase transition, which is compatible with the absence of thermal hysteresis related to the phase transition. X-ray diffraction experiments and magnetic measurements on field-oriented polycrystalline materials confirm the relatively strong magneto-crystalline anisotropy obtained at the Co rich side ($x = 3.5$, 3.75 and 4.0), with the c axis as the easy axis for the magnetisation direction and the a-b plane as the hard magnetic direction. The magnetocrystalline anisotropy constants are determined over a broad temperature range and show $K_2 > K_1 > 0$, in line with the easy direction for the magnetisation. Powder neutron diffraction experiments demonstrate the preference of Ni atoms for the 3g site. The magnetic properties are dramatically affected by the Ni/Co ratio. A dramatic decrease in the mean Co magnetic moment at the 3g site, the saturation magnetization and the Curie temperature was found for increasing Ni concentrations. The transition temperature T_C can be adjusted continuously over a broad temperature range for different Ni/Co ratios. This fulfils one important application requirement for the magnetocaloric materials. In this study, the evolution of the crystalline and magnetic structure, as well as changes in magnetic properties, are identified. They reveal large changes in the bulk physical properties, such as the magnetization, transport and thermal properties, which form the basis for their applications.

CRediT authorship contribution statement

N.H. van Dijk: Writing – review & editing, Supervision. **E. Brück:** Writing – review & editing, Supervision. **Wuliji Hanggai:** Writing – original draft, Software, Investigation.

Declaration of Competing Interest

The authors declare the following financial interests/personal relationships which may be considered as potential competing interests: W.Hanggai reports financial support was provided by Dutch Research Council. If there are other authors, they declare that they have no known competing financial interests or personal relationships that could have appeared to influence the work reported in this paper.

Data availability

Data will be made available on request.

Acknowledgements

References

[1] E. Brück, O. Tegus, D.T.C. Thanh, K.H.J. Buschow, J. Magn. Magn. Mater. 310 (2007) 2793–2799.
[2] J. Cui, M. Kramer, L. Zhou, F. Liu, A. Gabay, G. Hadjipanayis, B. Balasubramanian, D. Sellmyer, Acta Mater. 158 (2018) 118–137.
[3] J.M.D. Coey, Scr. Mater. 67 (2012) 524–529.
[4] O. Gutfleisch, M.A. Willard, C.H. Chen, E. Brück, S.G. Sankar, J.P. Liu, Adv. Mater. 23 (2011) 821–842.
[5] A.K. Pathak, M. Khan, K.A. Gschneidner, R.W. McCallum, L. Zhou, K. Sun, K. W. Dennis, C. Zhou, F.E. Pinkerton, M.J. Kramer, V.K. Pecharsky, Adv. Mater. 27 (2015) 2663–2667.
[6] A.V. Morozkin, A.V. Knotko, V.O. Yapaskurt, Fang Yuan, Y. Mozharivskyj, R. Nirmala, J. Solid State Chem. 208 (2013) 9–13.
[7] S.N. Klyamkin, V.N. Verbetsky, A.A. Karih, J. Alloy. Compd. 231 (1995) 479–482.
[8] A.V. Morozkin, Fang Yuan, Y. Mozharivskyj, O. Isnard, J. Magn. Magn. Mater. 368 (2014) 121–125.
[9] A.V. Morozkina, A.V. Garsheva, V.O. Yapaskurtc, J. Yao, R. Nirmala, S. Quezado, S. K. Malik, J. Solid State Chem. 265 (2018) 18–28.
[10] O. Isnard, Z. Arnold, N. Coroian, J. Kamarad, J. Magn. Magn. Mater. 316 (2007) 325–327.
[11] O. Moze, L. Pareti, A. Paoluzi, K.H.J. Buschow, Phys. Rev. B 53 (1996) 11550–11556.
[12] C.V. Thang, T.Q. Vinh, N.P. Thuy, J.J.M. Franse, Phys. B 246-247 (1998) 505–508.
[13] L. Pareti, M. Solzi, G. Marusi, J. Appl. Phys. 72 (1992) 3009.
[14] L. van Eijck, L.D. Cussen, G.J. Sykora, E.M. Schooneveld, N.J. Rhodes, A.A. van Well, C. Pappas, J. Appl. Cryst. 49 (2016) 1398–1401.
[15] H.M. Rietveld, J. Appl. Cryst. 2 (1969) 65–71.
[16] J. Rodriguez-Carvajal, Phys. B 192 (1993) 55–69.
[17] S. Legvold, in: Ferromagnetic Materials, North-Holland Publishing Company, Amsterdam, 1980, pp. 183–295.
[18] M. Pugaczowa-Michalska, M. Falkowski, A. Kowalczyk, Acta Phys. Pol. A 113 (2008) 323–326.
[19] C. Chacon, O. Isnard, J. Appl. Phys. 89 (2001) 71–75.
[20] V.K. Pecharsky, K.A. Gschneidner Jr., Phys. Rev. Lett. 78 (1997) 4494–4497.
[21] K.A. Gschneidner Jr., V.K. Pecharsky, A.O. Tsokol, Rep. Prog. Phys. 68 (2005) 1479–1539.
[22] V.K. Pecharsky, K.A. Gschneidner Jr., J. Appl. Phys. 86 (1999) 565–575.
[23] V. Franco, J.S. Blazquez, A. Conde, Appl. Phys. Lett. 89 (2006) 222512.
[24] J.Y. Law, V. Franco, L.M. Moreno-Ramírez, A. Conde, D.Y. Karpenkov, I. Radulov, K.P. Skokov, O. Gutfleish, Nat. Commun. 9 (2018) 2680.
[25] N.H. van Dijk, J. Magn. Magn. Mater. 529 (2021) 167871.
[26] C.V. Thang, L.H. Nam, N.P. Duong, N.P. Thuy, E. Brück, J. Magn. Magn. Mater. 196-197 (1999) 765–767.
[27] R.J. Caraballo Vivas, D.L. Rocco, T. Costa Soares, L. Caldeira, A.A. Coelho, M. S. Reis, J. Appl. Phys. 116 (2014) 063907.
[28] C. Zlotea, O. Isnard, J. Magn. Magn. Mater. 242-245 (2002) 832–835.
[29] C.V. Colina, O. Isnarda, M. Guillot, J. Alloy. Compd. 505 (2010) 11–16.

[30] L. Pareti, M. Solzi, G. Marusi, J. Appl. Phys. 72 (1992) 3009–3012.

[31] W. Sucksmith, F.R.S. Thompson, J.E. Thompson, Proc. R. Soc. A 225 (1954) 362.

[32] N. Coroian, V. Klosek, O. Isnard, J. Alloy. Compd. 427 (2007) 5–10.

[33] R.L. Streever, Phys. Rev. B. 19 (1979) 2704–2711.

[34] D. Benea, O. Isnard, N. Coroian, V. Pop, J. Magn. Magn. Mater. 322 (2010) 1052–1055.